© 2026. Published by The Company of Biologists | Journal of Cell Science (2026) 139, jcs264420. doi:10.1242/jcs.264420

RESEARCH ARTICLE

α-Ketoglutarate dehydrogenase complex activity modulates glutamate excitotoxicity via metabotropic regulation of NMDA receptors in primary cultures

Vanessa Goeschl[1,*], Matej Hotka[1,2,*], Bernhard Hochreiter[3], Karlheinz Hilber[1], Stefan Boehm[1], Andrey V. Kozlov[4] and Helmut Kubista[1,‡]

ABSTRACT

Glutamate excitotoxicity is a cell death mechanism triggered by accumulation of glutamate in the extracellular space. The α-ketoglutarate dehydrogenase complex (αKGDHC), an enzyme of the tricarboxylic acid cycle, represents a branching point controlling glutamate formation and its consumption as a fuel. Hence, modulation of the activity of αKGDHC might alter the amount of glutamate available for excitotoxic effects. To address this hypothesis, hippocampal neurons in primary co-culture with glial cells were exposed to zero-Mg^2 buffer to elicit excitotoxicity through N-methyl-D-aspartic acid (NMDA) receptor disinhibition. Pretreatment of the cultures with succinyl phosphonate, to inhibit αKGDHC, enhanced excitotoxity, whereas promotion of αKGDHC activity by pretreatment with thiamine caused an opposite action. Moreover, NMDA receptor currents – but not those mediated by α-amino-3-hydroxy-5-methyl-4-isoxazolepropionic acid (AMPA) receptors – were potentiated in neurons with impaired αKGDHC activity and diminished in neurons with boosted αKGDHC activity. The sensitization of NMDA receptors involved mGluR1 activation and was accompanied by enhanced neuronal discharge activity, elevated basal cytosolic Ca^{2+} levels, and augmented Ca^{2+} responses evoked by glutamate application. These results suggest that mGluR1-mediated potentiation of NMDA receptors contributes to a mechanism by which inhibition of αKGDHC might exacerbate glutamate excitotoxicity.

KEY WORDS: α-ketoglutarate dehydrogenase, Glutamate, Excitotoxicity, NMDA receptors, Hippocampus

INTRODUCTION

Glutamate is renowned as main excitatory neurotransmitter in the central nervous system (CNS). Nevertheless, glutamate subserves several additional functions in the CNS that are not limited to neurons (Nedergaard et al., 2002). One of the latter is its role as fuel for mitochondrial energy production; this necessitates entrance into the tricarboxylic acid (TCA) cycle after transformation to α-ketoglutarate which is further oxidized by the α-ketoglutarate dehydrogenase complex (αKGDHC), a rate-limiting step for the TCA cycle flux. Under pathophysiological conditions (e.g. ischemia, trauma, hypoglycemia, status epilepticus or neurodegenerative diseases), excessive release and accumulation of glutamate in the extracellular space can lead to overstimulation and induction of neuronal cell death, a mechanism known as glutamate excitotoxicity (Belov Kirdajova et al., 2020; Lewerenz and Maher, 2015; Olney, 1971). Owing to the role of glutamate in cell metabolism, glutamate might be distributed, in particular, between the αKGDHC-dependent oxidation and excessive efflux causing excitotoxicity (Divakaruni et al., 2017). This applies not only to glutamate in neurons but especially to glutamate in non-neuronal cells, such as astrocytes, which replenish neuronal glutamate via the glutamate-glutamine cycle (McKenna, 2007). This cycle is required for sustaining neuronal excitatory transmitter release (Tani et al., 2014).

In brain disorders, inhibition of αKGDHC can arise from increased production of reactive oxygen (ROS) and reactive nitrogen species (RNS) (Hansen and Gibson, 2022; Weidinger et al., 2023), which negatively impacts the flow of glutamate into and out of the TCA cycle. Hence, modulation of αKGDHC might potentially contribute to the pathophysiological effects of ROS and RNS. Succinyl phosphonate (SP) is a specific inhibitor of α-ketoglutarate dehydrogenase (αKGDH) and can be used as an experimental tool to study the block of αKGDHC (Bunik et al., 2005). Activation of αKGDH, by contrast, can be achieved by application of the co-factor precursor thiamine (TH) (Weidinger et al., 2023). The aim of this study was to investigate how a bidirectional modulation of αKGDHC activity by SP and TH following 36- to 48-h preincubation can affect glutamate excitotoxicity in primary hippocampal neuron and glia co-cultures. We hypothesized that inhibition of αKGDHC by SP might reduce the consumption of glutamate and thereby increase the availability of glutamate for excitotoxic effects as observed in neuroblastoma-derived cell lines (Weidinger et al., 2023). Vice versa, augmentation of αKGDHC activity by TH might boost glutamate consumption and thus reduce excitotoxicity.

Although SP was found to raise glutamate-mediated excitotoxicity, it failed to increase synaptic glutamate release. In turn, TH decreased glutamate excitotoxicity but enhanced synaptic glutamate release. These results exclude altered availability of synaptically releasable glutamate as underlying cause, and the data below hint at a modulation of N-methyl-D-aspartic acid (NMDA) receptors through activation of metabotropic glutamate receptor signaling.

[1]Center of Physiology and Pharmacology, Department of Neurophysiology and Neuropharmacology, Medical University of Vienna, 1090 Vienna, Austria. [2]Department of Physiology, Faculty of Medicine, Faculty of Medicine, Karl Landsteiner University, 3500 Krems, Austria. [3]Institute of Science and Technology Austria, Imaging and Optics Facility, 3400 Klosterneuburg, Austria. [4]Ludwig Boltzmann Institute for Traumatology, The Research Center in Cooperation with AUVA, Vienna, Austria.
*These authors contributed equally to this work

‡Author for correspondence (helmut.kubista@meduniwien.ac.at)

H.K., 0000-0002-5805-8649

Handling Editor: Subhojit Roy
Received 3 September 2025; Accepted 4 March 2026

Journal of Cell Science (2026) 139, jcs264420. doi:10.1242/jcs.264420

RESULTS

Effect of αKGDHC modulation on zero-Mg^{2+}-induced excitotoxicity

Hippocampal neuron and glia co-cultures were exposed for 6 h to an external solution without added Mg^{2+} ('zero-Mg^{2+}'), a treatment that causes excess glutamatergic neuronal activity (Meyer et al., 2021) and widespread neuronal death (Kovac et al., 2012). Afterwards, the neuronal viability was investigated by fluorescence staining of dead neurons in the cultures with propidium iodide (PI) (Fig. 1A). A schematic representation of the experimental procedure can be found in Fig. S1. Under control conditions (ctrl), this treatment reduced neuronal viability to ∼50% (48.8±5.4%, mean±s.d.). In cultures that had been pretreated for 36 to 48 h with 200 µM SP, viability was reduced even more to ∼40% (41.4±4.5%). In contrast, pretreatment of cultures for the same period of time with 1 mM TH led to enhanced viability of ∼65% (63.1±4.8%). In other words, zero-Mg^{2+}-induced excitotoxicity killed ∼25% more neurons in cultures pretreated with SP versus in those pretreated with TH. Notably, changes in viability caused by either SP or TH as compared with control were lost when both compounds were combined during pretreatment. When neurons were incubated in (Mg^{2+}-containing) standard external solution (denoted unstimulated cultures), neuronal viability was high (ctrl, 93.6±2.7%; mean±s.d.) and remained largely unaltered irrespective of whether cultures where pretreated with TH (92.0±2.5%) or the combination of both SP+TH (92.4±2.6%) (Fig. 1B). However, after pretreatment with SP, neuronal viability was reduced to 88.2±5.4%, which was significantly different from the other pretreatment groups (Fig. 1B).

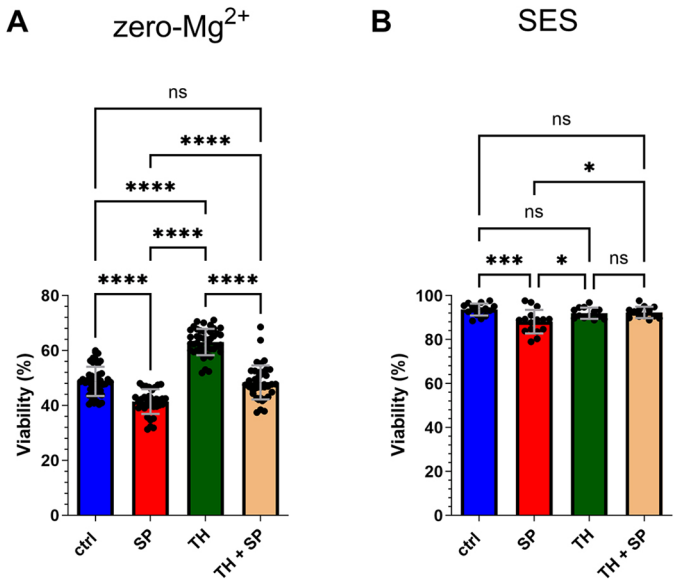

Fig. 1. Modulation of αKGDHC activity affects zero-Mg^{2+}-induced excitotoxicity. (A) Bar graphs (depicting mean±s.d. together with the individual data points) of neuronal viability determined after exposure to zero-Mg^{2+}-induced excitotoxicity of untreated cultures (ctrl, *n*=45), cultures pretreated for 36 to 48 h with SP (*n*=36), with TH (*n*=42) or with both compounds (TH+SP, *n*=41) (from three independent culture preparations). (B) Bar graphs of neuronal viability observed in unstimulated cultures (after exposure to Mg^{2+} standard external solution (SES)] for neurons without or with pretreatment as in A (ctrl *n*=15, SP *n*=16, TH *n*=13, TH+SP *n*=13, from one culture preparation, three dishes per condition). *P<0.05; ***P<0.001; ****P<0.0001; ns, not significant (ordinary one-way ANOVA in combination with Tukey's multiple comparisons post hoc test).

Effect of αKGDHC modulation on vesicular glutamate release

In cortical neurons, a switch in metabolic preference from pyruvate to glutamate has been shown to decrease currents evoked by hyperosmotic sucrose, indicating that the quantity of glutamate released upon depolarization was diminished (Divakaruni et al., 2017). We confirmed this finding in our rat hippocampal primary cultures (Fig. S2). Likewise, activation and inhibition of αKGDHC by TH and SP, respectively, might alter levels of glutamate in synaptic vesicles. To test for this possibility, we also employed the hyperosmotic sucrose assay to evaluate vesicular glutamate (Rosenmund and Stevens, 1996). A graphical explanation of this assay is provided in Fig. S3. 500 mM sucrose-containing external solution was superfused onto patch-clamped neurons for 10 s and current responses were monitored (Fig. 2A). Analysis of peak current densities (ctrl, 6.3±3.8 pA/pF; SP, 3.3±0.8 pA/pF; TH, 9.9±3.8 pA/pF; mean±s.d.) of evoked responses indicated a trend towards reduced glutamate contents in synaptic vesicles of SP-pretreated neurons, although this change did not reach statistical significance (P-value 0.1482). However, in TH-pretreated neurons, evoked responses were significantly larger than in untreated neurons and SP-pretreated neurons (Fig. 2B). No statistically significant difference was present in membrane capacitance (the mean capacitance amounted to ∼75 pF) between the investigated pretreatment groups (Fig. 2C).

These data provide evidence for a particularly high glutamate content in synaptic vesicles after TH pretreatment and a considerably smaller content of glutamate in vesicles pretreated with SP. However, they do not support the idea that enhanced availability of glutamate for synaptic release upon inhibition of αKGDHC-dependent consumption is responsible for the augmented zero-Mg^{2+}-induced excitotoxicity seen in SP-pretreated neurons. Likewise, they do not support the idea that lowered availability of glutamate for synaptic release upon promotion of αKGDHC-dependent consumption is responsible for the reduced excitotoxicity seen in TH-pretreated neurons. Therefore, we turned our focus from presynaptic actions to postsynaptic ones.

Effect of αKGDHC modulation on glutamate-induced excitotoxicity

First, we investigated whether modulation of αKGDHC could also alter excitotoxicity caused by exogenous application of glutamate in a manner similar to that caused by zero-Mg^{2+}. We used different glutamate concentrations and application periods to induce varying degrees (∼10 to 45%) of neuronal cell death (Fig. 3). A schematic representation of the experimental procedure can be found in Fig. S4. Similar to the zero-Mg^{2+} experiments, we also observed increased excitotoxicity in SP-pretreated neurons, particularly – and here the effect was statistically significant – when 10 µM glutamate was administered. In comparison, TH-pretreated neurons showed reduced excitotoxicity compared to SP-pretreated neurons, which was statistically significant at all glutamate concentrations tested. When neurons were pretreated with both SP and TH, no increase in cell death was observed (Fig. 3). Taken together, the findings so far appear to show that changes in excitotoxicity depend more on how the neurons respond to glutamate rather than how much they release.

Effect of αKGDHC modulation on glutamate-induced neuronal excitation

To address this possibility, we applied increasing concentrations of glutamate (3 to 300 µM) for periods of 2 min with equally long intervals to patch-clamped neurons and performed current clamp recordings to monitor membrane voltage (V_m) responses (Fig. 4A).

Journal of Cell Science (2026) 139, jcs264420. doi:10.1242/jcs.264420

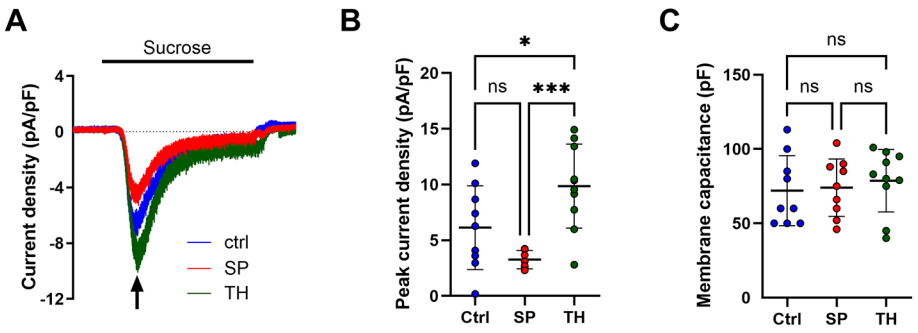

Fig. 2. Modulation of αKGDHC activity affects hyperosmotic sucrose-induced currents. (A) Averaged currents (normalized to the cell capacitance as a proxy for cell size and representing mean values) from 9 or 10 neurons evoked by 10 s-long application of 500 mM sucrose-containing external solution from cultures with unaltered αKGDHC activity (cntl, blue trace), and from cultures pretreated with SP (red trace) and from cultures pretreated with TH (green trace), both for 36 to 48 h. For clarity, brief application artefacts at the beginning and at the end of the sucrose application were removed from the traces. The arrow indicates the peaks of evoked currents. (B) Plot of peak current densities (peaks of currents indicated in A by the arrow) together with the mean±s.d. from responses recorded from 9 to 10 neurons in each of the three conditions. (C) Plot of the membrane capacitance as correlate of cell size determined in the neurons from which data in B were assembled and which was used to normalize the currents shown in A with mean±s.d. *P<0.05; ***P<0.001; ns, not significant (ordinary one-way ANOVA in combination with Tukey's multiple comparisons post hoc test).

The V_m traces obtained reveal differences in endogenous discharge behavior between cultures that had been exposed to distinct pretreatments (Fig. 4A–C), but these changes are disregarded here, and will be examined in more detail below. Glutamate-induced depolarizations were determined only in between single action potentials (using baseline values) or after the onset of depolarization block (cessation of action potentials in the course of persistent depolarization); concentration response curves were generated in order to obtain an initial insight into potential changes in glutamate-induced excitation (Fig. 4D). Compared to controls (black trace, n=6), neurons pretreated with SP (red trace, n=3) responded to lower concentrations of glutamate, whereas TH-pretreated neurons (green trace, n=7) required higher glutamate concentrations to respond. The effect of SP (red trace) was prevented by co-application of TH (SP+TH, orange trace, n=6). From the Hill slope model fitted to the data, EC_{50} values were determined as 18.1 µM (ctrl), 8.7 µM (SP), 38.3 µM (TH) and 26.2 µM (SP+TH). A preliminary statistical evaluation of the fitted concentration–response curves revealed that the EC_{50} values from the four groups were not drawn from the same underlying population distribution (Fig. 4D). To corroborate the increased sensitivity of SP-pretreated neurons to low concentrations of glutamate, we repeated these experiments for 3 µM and 10 µM glutamate in a larger cohort of neurons and preparations (n=15 to 19 neurons from six or seven different preparations; Fig. 5A). Instead of using the depolarized voltage value (as in the previous figure, where V_m indicates the absolute potential to which neurons depolarized), here we evaluated ΔV_m, defined as the difference between the depolarization reached in the presence of glutamate (the

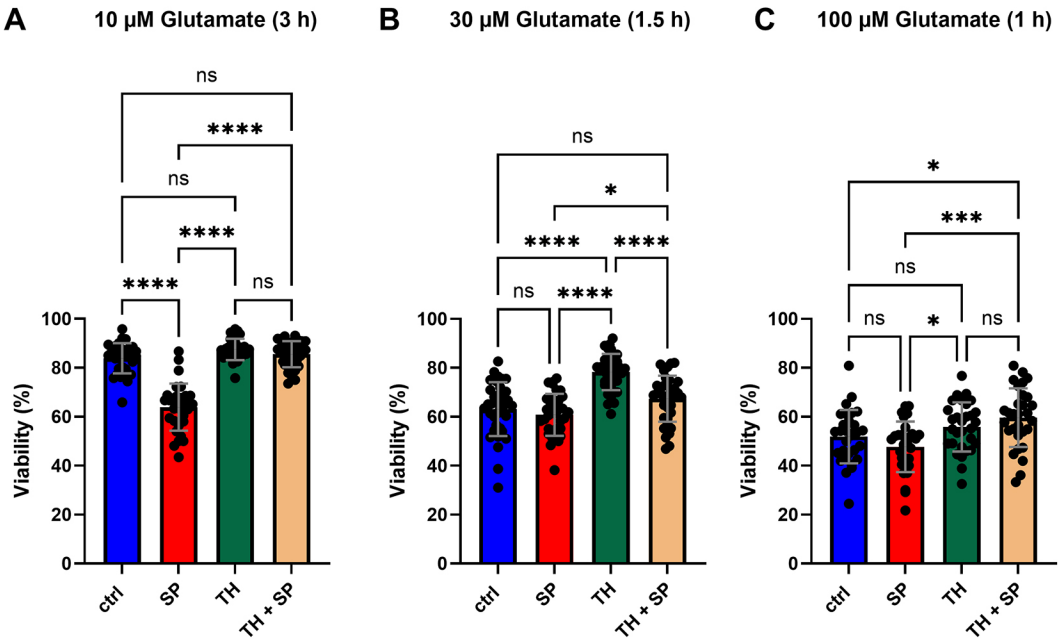

Fig. 3. Modulation of αKGDHC activity affects glutamate excitotoxicity. (A) Bar graphs (depicting mean±s.d. together with the individual data points) of neuronal viability determined 24 h after 3-h exposure to 10 µM glutamate of untreated cultures (ctrl), cultures pretreated for 36 to 48 h with SP, with TH or with both compounds (TH+SP) (n=32 for each condition). (B) Same as in A after a 1.5-h exposure to 30 µM glutamate (n=36 for each condition). (C) Same as in A after a 1-h exposure to 100 µM glutamate (n=30 for each condition). All data were collected from three independent culture preparations. *P<0.05; ***P<0.001; ****P<0.0001; ns, not significant (ordinary one-way ANOVA in combination with Tukey's multiple comparisons post hoc test).

Journal of Cell Science (2026) 139, jcs264420. doi:10.1242/jcs.264420

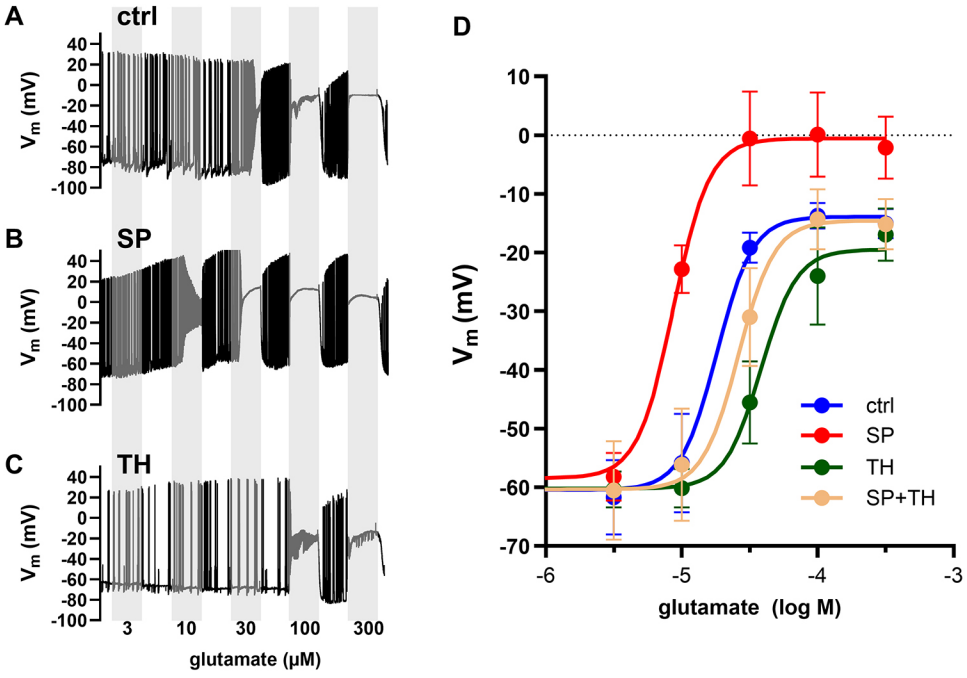

Fig. 4. Concentration-response relationship of glutamate-evoked neuronal depolarizations. (A–C) Examples of current clamp recordings from a neuron with unaltered αKGDHC activity (ctrl, A), from a neuron pretreated with SP (B) and from a neuron pretreated with TH (C). The 2-min long application of increasing concentrations of glutamate is indicated by gray vertical bars (from left to right: 3, 10, 30, 100 and 300 μM). (D) Concentration–response curves of glutamate-evoked depolarizations recorded from 3 to 7 neurons in each of the three conditions illustrated with sample recordings in A–C, as well as from neurons pretreated with a combination of SP and TH. Data are presented as mean±s.e.m. The colored curves were generated using a non-linear fit routine. Comparison of fits of the concentration–response curves indicated a statistically significant difference in EC_{50} values between one dataset and the remaining conditions (P=0.0008, extra sum-of-squares F test). The coefficient of determination (R^2) values were 0.772 for the control group, 0.895 for SP, 0.652 for TH and 0.612 for SP+TH.

lowest V_m during glutamate application) and the membrane voltage immediately before glutamate application (the resting V_m). Thus, ΔV_m indicates the size of the glutamate-induced depolarizations. In SP-pretreated neurons, the responses evoked by 3 μM glutamate (21.2±10.6 mV, mean±s.d.) were significantly larger than the responses evoked in control neurons (7.3±7.3 mV) and in TH-pretreated neurons (5.8±6.7 mV). A similar effect was seen with 10 μM glutamate, although the difference between control neurons (31.1±19.3 mV) and SP-treated neurons (42.8±12.1 mV) did not reach statistical significance (Fig. 5B). The responses to 10 μM glutamate in TH-treated neurons amounted to 20.2±16.0 mV, and were significantly different from the responses evoked in SP-treated neurons.

As mentioned above, the current clamp recordings provide evidence of a further difference (besides the sensitivity to glutamate) between the three pretreatment groups – that is, we noted a higher likeliness of pronounced discharge activity in SP-treated neurons, whereas TH-treated neurons seemed to display reduced discharge activity (Figs 4 and 5). To evaluate this observation, we defined five discharge patterns in the sections of the recordings that preceded the first application of glutamate, as illustrated in the exemplar recordings in Fig. 6A. First, silent neurons, which showed – within 1-min time frames after the start of recordings – excitatory synaptic potentials but did not display action potential firing (‘silent’). Second, predominantly silent neurons that showed irregular discharge of a few individual action potentials (‘silent+Aps’). Third, neurons that showed continuous discharge of action potentials in a 1-min recording period (‘continuous firing’). Forth, neurons that also showed a high likeliness of action potentials but in which action potentials occurred in a discontinuous fashion with periods of frequent discharge (e.g. 4 to 7 Hz) separated by pauses of firing (‘discontinuous firing’). And finally, fifth, neurons which showed ‘burst firing’ in which depolarizing waves gave rise to alternating periods of high frequency discharge firing and of discharge pauses.

Next, we allocated neurons of the three pretreatment groups (ctrl, n=32; SP, n=43; TH, n=45) to these five discharge patterns. Results

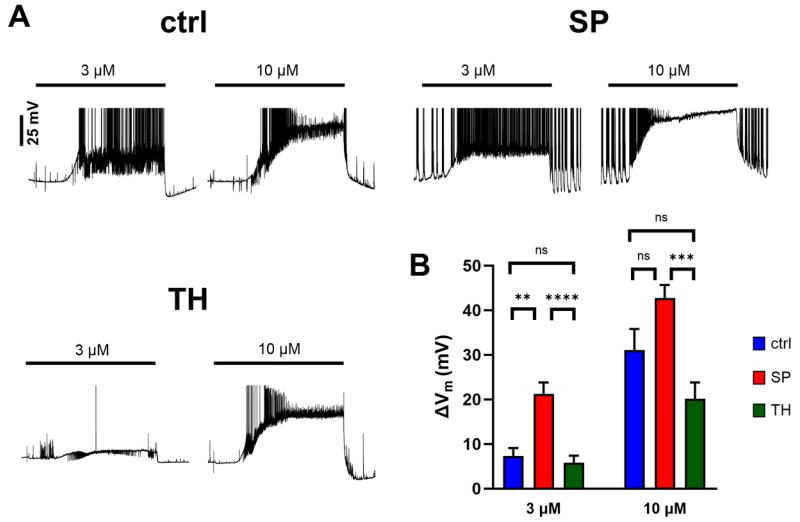

Fig. 5. Effect of αKGDHC modulators on depolarizing voltage responses evoked by application of low concentrations of glutamate. (A) Depiction of representative voltage responses to application of 3 μM and 10 μM glutamate of control neurons, SP-treated neurons and TH-treated neurons. Responses were characterized by triggering of or increase in action potential discharge, and at 10 μM glutamate, by a transition into depolarisation block, which manifests itself in a cessation of discharge activity during sustained depolarization. Action potentials are truncated at −10 mV. (B) Bar graph (mean+s.e.m.) illustrating the differences between voltage responses (ΔV_m) to glutamate application in the three pretreatment groups. **P<0.01; ***P<0.001; ****P<0.0001; ns, not significant (Kruskal–Wallis test with Dunn’s multiple comparisons post hoc test).

Journal of Cell Science (2026) 139, jcs264420. doi:10.1242/jcs.264420

A

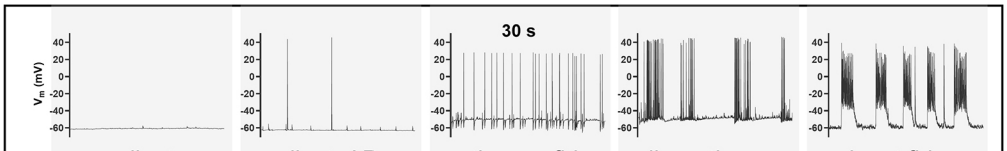

	silent	silent+APs	continuous firing	discontinuous	burst firing
ctrl	12% (4/32)	**31% (10/32)**	10% (3/32)	**31% (10/32)**	16% (5/32)
SP	7% (3/43)	19% (8/43)	12% (5/43)	**39% (17/43)**	23% (10/43)
TH	22% (10/45)	**42% (19/45)**	4% (2/45)	31% (14/45)	0% (0/45)

B

ctrl	**53% (17/32)**	47% (15/32)
SP	37% (16/43)	**63% (27/43)**
TH	**69% (31/45)**	31% (14/45)

Fig. 6. Distribution of neuronal discharge patterns according to αKGDHC activity. (A) 30 s recording periods illustrating the discharge pattern categories defined for the analysis. The values below indicate the percentage and – in brackets – numbers of neurons in which the respective discharge pattern was observed out of the total number of neurons investigated. (B) Same as in A but only for hypoactive neurons (comprising the three discharge patterns indicated on the left side) and for hyperactive neurons (comprising the two discharge patterns indicated on the right side). Bold font in A and B highlights the predominant (i.e. most frequent) discharge pattern in the respective pretreatment group.

of this analysis are presented in Fig. 6A,B. In control neurons, the predominating discharge patterns (indicated in bold) were 'silent+Aps' and 'discontinuous firing'. In SP-treated neurons, discontinuous discharge activity was the predominant pattern. Finally, in TH-treated neurons, 'silent+Aps' represented the predominant discharge pattern (Fig. 6A). To highlight the differences in discharge activity, we pooled hypoactive discharge patterns (first to third categories) and hyperactive discharge patterns (fourth and fifth categories) (Fig. 6B). In control neurons, hypoactive discharge patterns and hyperactive discharge patterns were found with almost equal probability. However, in SP-treated neurons about two thirds of the neurons displayed hyperactivity, whereas about one third of the neurons were characterized by hypoactivity. The situation in TH-treated neurons was exactly the opposite, in that about two thirds of the neurons displayed hypoactivity, whereas about one third of the neurons were characterized by hyperactivity. At the same time, there was no statistically significant difference in the resting membrane potential among the three pretreatment groups, which amounted to −62.1 ±9.3 mV in control neurons, to −63.3±10.5 in neurons pretreated with SP and to 65.7±9.9 mV (mean±s.d.) in neurons pretreated with TH.

Effects of αKGDHC modulation on NMDA- and AMPA-induced currents

To explore the molecular origin of altered sensitivity to glutamate in neurons preincubated with SP or TH, we next investigated the effects of αKGDHC modulation on ionotropic glutamate receptors. We applied either 3 µM AMPA or 30 µM NMDA to voltage-clamped neurons to evoke glutamate receptor-mediated currents. These concentrations correspond approximately to the EC_{50} values for these compounds in our culture system, as can be seen for NMDA-induced currents in Fig. 7C [as for AMPA, currents elicited with 3 µM amounted to 10.30±4.13 pA/pF (mean±s.d., n=9); at 300 µM, AMPA currents amounted to 17.21±4.60 pA/pF, which was not significantly different (P-value 0.43, paired t-test) from the AMPA currents evoked with 100 µM (16.89±4.89 pA/pF); hence 300 µM can be considered to represent a saturating concentration, and with 3 µM AMPA 59.8% of the maximal current at 300 µM was elicited. These data are in line with previous reports on the respective EC50 values by, for example, Banke and Lambert, 1999; Fukushima et al., 2014 and Herman and Jahr, 2007]. Densities of AMPA-induced currents did not reveal any significant differences between the four experimental groups (control, SP-treated, TH-treated and SP+TH-treated neurons) (Fig. 7A). In contrast, compared to controls, neurons pretreated with SP showed increased densities and neurons pretreated with TH reduced densities of NMDA-evoked currents. No change of NMDA-induced currents was evident from the data of neurons pretreated with a combination of SP and TH (Fig. 7B). Both, the increase in SP-treated neurons as well as the decrease in TH-treated neurons showed statistically significant. In concentration response curves obtained with 3 to 300 µM NMDA (Fig. 7C), EC_{50} values were similar for the four groups of differentially pretreated neurons (control 22.5 µM, SP 22.1 µM, TH 27.7, and SP+TH 24.4 µM). Maximal current densities, in contrast, were reduced by TH and enhanced by SP (Fig. 7C).

Involvement of metabotropic glutamate receptors

Activation of group I metabotropic glutamate receptors (mGluRs) are known to potentiate NMDA receptor responses (Fitzjohn et al., 1996; Skeberdis et al., 2001). Hence, we tested whether antagonizing mGluR1 and mGluR5 receptors (encoded by *GRM1* and *GRM5*, respectively) would affect the SP-induced increase of NMDA receptor currents. As summarized in the plot of peak current densities in Fig. 8A, the SP-induced increase in NMDA receptor currents was entirely blocked in the presence of the mGluR1 antagonist YM298198 (YM, 1 µM). In contrast, the mGluR5 antagonist MTEP (1 µM) failed to significantly attenuate facilitatory effects of SP, even though NMDA receptor currents were enhanced when compared to control conditions. These data indicate that inhibition of αKGDHC by SP in hippocampal cultures leads to a mostly mGluR1-mediated potentiation of NMDA receptor responses. To reveal whether this sensitization of NMDA receptors might be related to the reduced viability of SP pretreated neurons in zero-Mg^{2+} (Fig. 1) or glutamate-induced excitotoxicity (Fig. 3), we investigated glutamate-induced cytosolic Ca^{2+} elevations using the fluorescent Ca^{2+} indicator Fluo4. Tetrodotoxin (TTX, 0.5 µM) and the phospholipase C inhibitor U73122 (1 µM) were included in the buffer to avoid network effects and the effects of phospholipase C activation downstream of group I mGluRs. In comparison to control conditions, cytosolic Ca^{2+} rises in response to 1-min applications of 10 µM glutamate were higher in SP-treated neurons and were accompanied by signs of Ca^{2+} dysregulation – for example, compromised return to baseline levels after wash-out of glutamate, in some (Fig. 8B, red trace) but not all of the neurons

Journal of Cell Science (2026) 139, jcs264420. doi:10.1242/jcs.264420

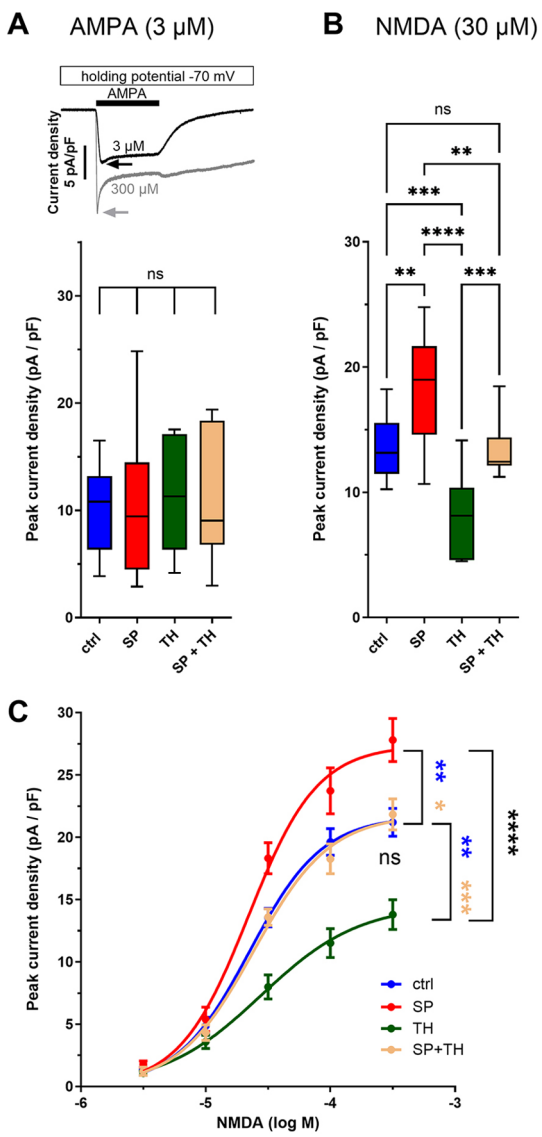

Fig. 7. Effect of αKGDHC modulation on AMPA- and NMDA-evoked currents. (A) The traces at the top show representative currents elicited with 3 µM AMPA, and – for comparison – 300 µM AMPA. The 5-s application of AMPA onto neurons voltage-clamped to a holding potential of −70 mV is indicated by the black horizontal bar. Owing to the normalization to the cell capacitance (as a proxy for cell size), data are referred to as current density. The arrows indicate peaks of the currents. Those evoked with 3 µM AMPA were used for the analysis depicted in the box-and-whisker plot below. The plot shows a comparison of peak current densities of currents elicited by 3 µM AMPA in control neurons (ctrl) versus neurons pretreated with SP (red bar), TH (green bar) or SP+TH (orange bar); *n*=9 for each pretreatment group. The box spans from the 25th percentile to the 75th percentile, representing the interquartile range. The line inside the box marks the median. The whiskers indicate minimum and maximum values. (B) Same as in A but for peak current densities of currents elicited by a 5-s-long application of 30 µM NMDA; *n*=11 for each pretreatment group. (C) Concentration–response curves for peak current densities evoked by increasing concentrations of NMDA in the four indicated pretreatment groups; *n*=11 for each concentration in each pretreatment group. Data points represent the mean±s.e.m. Statistical evaluation of the data obtained with 300 µM NMDA is indicated on the right side. The colored asterisks indicate whether comparison refers to control data (blue) or data from SP+TH-treated neurons (orange). The colored curves were generated by a non-linear fit routine with the bottom constrained to 0. R squared values were as follows: ctrl 0.899, SP 0.845, TH 0.736 and SP+TH 0.884. **P*<0.05; ***P*<0.01; ****P*<0.001; *****P*<0.0001; ns, not significant (ordinary one-way ANOVA in combination with Tukey's multiple comparisons post hoc test).

(Fig. 8C, red trace). Moreover, baseline Ca^{2+} was increased in SP-treated neurons as well (Fig. 8D). Both of these effects of SP, enhancement of baseline Ca^{2+} and glutamate-induced Ca^{2+} rises were prevented by co-administration of TH (Fig. 8B) or of the mGluR1 antagonist YM298198 (Fig. 8C, YM). The data are summarized in bar graphs of Fig. 8D (baseline Ca^{2+}) and Fig. 8E (peak Ca^{2+}-evoked by 10 µM glutamate). Baseline Ca^{2+} and peak Ca^{2+} responses were only larger than those registered under control conditions for SP-treated neurons. In all other pretreatment groups, baseline Ca^{2+} and peak Ca^{2+} responses were smaller in size than those registered under control conditions. These data demonstrate that TH as well as YM prevented the Ca^{2+}-elevating effect of SP treatment both at rest and during glutamatergic stimulation.

DISCUSSION

Inhibition of αKGDHC leads to an mGluR1-dependent potentiation of NMDA receptors

For energy production via the TCA cycle of neurons and glial cells, αKGDHC is required to convert α-ketoglutarate into succinyl-CoA. Alternatively, α-ketoglutarate can be used for the synthesis of glutamate, a reaction that is found primarily in astrocytes (Alcoreza et al., 2021). Glutamate is either released from astrocytes via several pathways (reviewed by Mahmoud et al., 2019) or transformed into glutamine to reach neurons via the glutamate-glutamine cycle (McKenna, 2007). In neurons, glutamine-derived glutamate is either loaded into vesicles for exocytotic release or utilized for energy production. Inhibition of αKGDHC can be expected to boost the formation of glutamate from α-ketoglutarate in astrocytes. There, only a minor fraction of glutamate (~15%) is fed into the TCA cycle, and ~85% is transferred to neurons (Alcoreza et al., 2021). Hence, raised astrocytic glutamate might potentially result in elevated levels of extracellular glutamate through enhanced exocytosis from neuronal vesicles. Indeed, αKGDHC inhibition by SP in a neuron–glia hybrid cell line has been reported to redirect the flow of glutamate into a reserve vesicle pool with ensuing accumulation of extracellular glutamate after spontaneous release. This mechanism was suggested to directly favor excitotoxic effects and to provoke cell death, but the effects were only seen when a neuron-like cell line was exposed to millimolar concentrations of exogenously added glutamate (Weidinger et al., 2023).

In the present experiments on primary neuron and glia co-cultures, basal viability was reduced and excitotoxicity due to disinhibition of NMDA receptors through Mg^{2+} removal was augmented by the αKGDHC inhibitor SP, and both effects were occluded by co-administration of the αKGDHC co-factor precursor TH. Nevertheless, glutamate release was not altered in a way supporting enhanced vesicular release as the cause of increased excitotoxicity in SP-pretreated neurons. Sucrose-induced glutamate release was higher in TH-treated neurons than in SP-treated ones, even though excitotoxicity was lowest in TH-treated and highest in SP-treated cultures. Instead, SP treatment resulted in a TH-sensitive and mGluR1-dependent sensitization of NMDA receptors. This suggests that the source of glutamate that led to an augmentation of cell death was a non-synaptic rather than a synaptic one, which sufficed to activate mGluR1 receptors (which have an affinity for glutamate in the submicromolar range; Tora et al., 2018), which mediate an increase in NMDA receptor sensitivity.

Inhibition of αKGDHC causes neuronal hyperactivity, enhancement of cytosolic Ca^{2+} and a reduction of viability

mGluR1-mediated potentiation of NMDA receptors is a well-known mechanism in hippocampal neurons (Benquet et al., 2002; Fitzjohn

Journal of Cell Science (2026) 139, jcs264420. doi:10.1242/jcs.264420

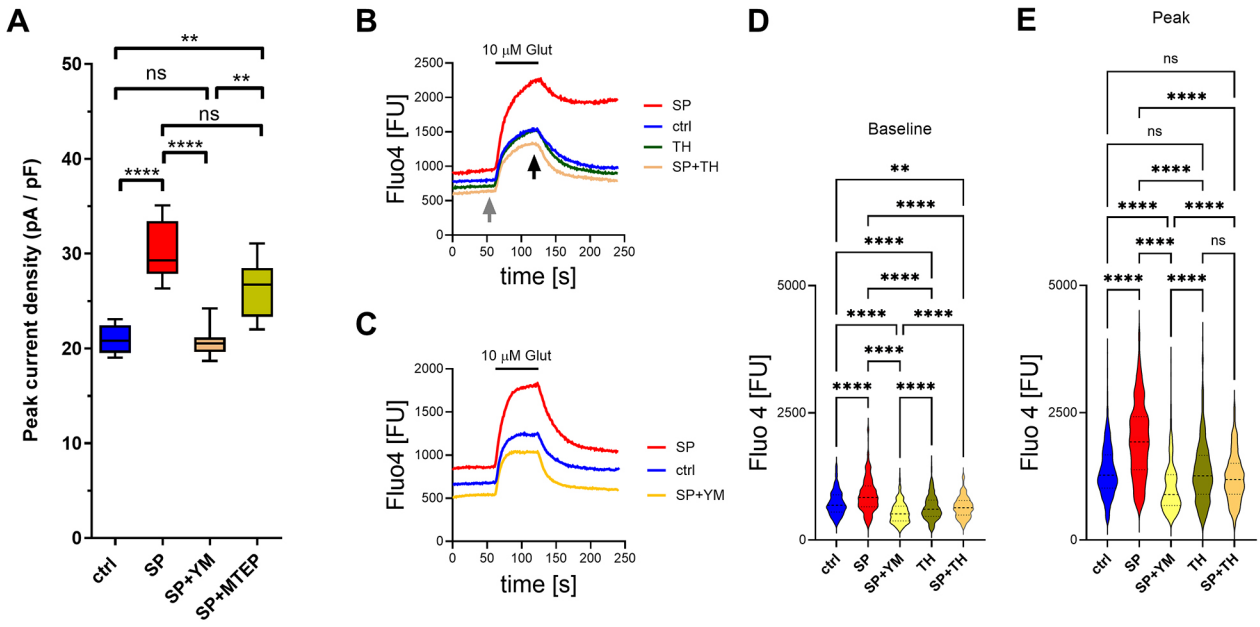

Fig. 8. Effects of αKGDHC inhibition by SP involve mGluR1 activation. (A) Box-and-whisker plot (as in Fig. 7) illustrating the effect of SP treatment or of SP treatment in the presence of the group I mGluR antagonists YM298198 (mGluR1 antagonist) or MTEP (mGluR5 antagonist) on peak current densities of currents evoked by 300 µM NMDA (n=5–7 for the four different conditions). **P<0.01; ****P<0.0001; ns, not significant (ordinary one-way ANOVA in combination with Tukey's multiple comparisons post hoc test). (B) Comparison of averaged traces (representing the mean) obtained during Fluo4 registration of cytosolic Ca^{2+} before, during and after application of 10 µM glutamate (Glut) from neurons pretreated with SP (n=110), TH (n=120) or TH+SP (n=115), or from untreated neurons (ctrl, n=154). (C) Comparison of averaged traces (representing the mean) obtained during Fluo4 registration of cytosolic Ca^{2+} from neurons pretreated with SP (n=217), SP+YM298198 (YM, 1 µM) (n=277) or from untreated neurons (ctrl, n=221). (D) Violin plot summarizing baseline Ca^{2+} signals determined prior to the glutamate application (marked in B with the gray arrow) in experiments as illustrated in B and C, together with an indication of the results of statistical comparison of the various pretreatment groups (n=277–375 neurons from four dishes, one dish per pretreatment group, three microscopic fields per dish, repeated in a total of four preparations). The median value is indicated as a line within the violin. The first and third quartiles are indicated by additional lines. (E) Same as in D but for the peak Ca^{2+} signals determined during the application of 10 µM glutamate (marked in B with the black arrow). **P<0.01; ****P<0.0001; ns, not significant (Kruskal–Wallis test with Dunn's multiple comparisons post hoc test). FU, fluorescence units.

et al., 1996; Lan et al., 2001; Skeberdis et al., 2001). However, pretreatment of neurons with SP and/or TH also affected their firing properties, and SP-treated neurons were hyperactive, whereas TH-treated neurons were hypoactive. In particular, burst discharge was absent in TH-treated neurons, but the number of neurons displaying burst firing was increased after SP treatment. As NMDA receptors are known as key regulators of burst firing in hippocampal neurons (Grienberger et al., 2014; Teplov et al., 2021), this change in discharge pattern might result directly from alterations in NMDAR sensitivity. Changes in discharge modes other than burst firing might be viewed as consequence of an altered number of bursting neurons within a network. However, we cannot exclude that additional changes induced by the modulation of αKGDHC activity could also play a role in the shift of discharge behavior. Still, higher firing rates in networks of SP-treated neurons might suffice to explain enhanced cytosolic Ca^{2+} concentrations as revealed in Fluo4 experiments as well as reduced viability of neurons even in the absence of a zero-Mg^{2+} challenge.

mGluR1-dependent potentiation of NMDA receptors might represent a pathomechanism associated with reduced activity of αKGDHC

The mechanisms underlying the sensitization of NMDA receptors via mGluR1 have not been the focus of this study. Previously, mGluR1-mediated insertion of NMDARs (Lan et al., 2001) as well as tyrosine-phosphorylation of membrane-resident receptors (Heidinger et al., 2002; Murotomi et al., 2008) have been implicated.

The activity of αKGDHC is decreased in many neurodegenerative disorders (Starkov, 2013), and inhibition of αKGDHC can arise from an increased production of ROS and RNS in brain pathology (Hosmann et al., 2021; Hansen and Gibson, 2022). Furthermore, TH deficiency is well known to cause neuronal vulnerability via glutamate-mediated excitotoxic mechanisms (Nardone et al., 2013). Hence, we propose that the mechanism described here in primary hippocampal neuron and glia co-cultures might play a role in diseases associated with reduced activity of αKGDHC. Indeed, evidence has been provided that group I mGluRs potentiate both post-traumatic and ischemic glutamate excitotoxicity, and that this effect involves upregulation of NMDA receptor activity (Lai et al., 2019; Mukhin et al., 1996 and 1997). Moreover, infarct volume is reduced by the action of mGluR1 antagonists in rodent ischemia models (Kohara et al., 2008; Li et al., 2013). Murotomi et al. (2008) report similar findings and demonstrate that a reduction of NMDA receptor (NMDAR) function is associated with this neuroprotective effect. Our *in vitro* data indicate that inhibition of αKGDHC leads to mGluR1-dependent potentiation of NMDAR signaling that has low neurotoxic effects on its own (and might thus be caused by mild increases of extracellular glutamate), but renders neurons more susceptible to excitotoxic effects of glutamate surges. The ischemic penumbra, a region of brain tissue that is not immediately irreversibly damaged, but which is at risk for secondary injury, is highly susceptible to oxidative stress (Hou and Brenner, 2024), which might lead to reduced αKGDHC activity (Hansen and Gibson, 2022; Weidinger et al., 2023). Therefore, we propose that mGluR1-mediated potentiation of NMDA receptors represents a mechanism

Journal of Cell Science (2026) 139, jcs264420. doi:10.1242/jcs.264420

that might contribute to the spreading of a precipitating (e.g. ischemic) brain lesion.

It should be noted that acute application of SP has been demonstrated to cause neuroprotective rather than excitotoxic effects in cerebellar granule neurons. There, a 1-hour pre-application of SP has been shown to alleviate Ca^{2+} dysregulation evoked by 30 min application of 100 µM glutamate. As the underlying mechanism, the authors inferred prevention of αKGDHC-dependent ROS production and ensuing self-inactivation of αKGDH (upon overstimulation of neurons with glutamate) (Bunik et al., 2009; Kabysheva et al., 2009). In our study, we investigated effects of long-term (e.g. 36 to 48 h long) inhibition of αKGDHC, a condition under which changes in ambient glutamate were hypothesized to arise and to affect neuronal function in a manner different from immediate effects of reduced αKGDHC activity.

Inhibition of glutamate receptors and augmentation of glutamate uptake into glial cells have been proposed as strategies to reduce glutamate excitotoxicity (Wang et al., 2020). However, reduction of glutamate signaling will inevitably impair brain function. Hence, additional or alternative strategies leading to neuroprotection from the toxic effects of excess glutamate are needed. Understanding the role of glutamate metabolism in excitotoxicity shall help to identify targeted strategies for therapeutic intervention with deleterious effects of extracellular glutamate accumulation. Meanwhile, current evidence strongly supports the therapeutic use of TH supplementation to improve outcomes in moderate to severe traumatic brain injury (Gao et al., 2025; Wang et al., 2024). The results of our study propose a mechanism by which restoration of impaired activity of αKGDHC might be partially responsible for the mitigating effect of TH supplementation on brain damage.

Limitations

Thiamine pyrophosphate, the active form of TH to which it is rapidly converted by thiamine pyrophosphokinase, acts as a cofactor for several enzymes – for example, pyruvate dehydrogenase, transketolase and branched-chain α- ketoacid dehydrogenase – as well as αKGDH (Hamada et al., 2013). Hence, the effects of TH can be attributed to a modulation of a variety of enzymes. However, the effect of SP on αKGDH is considered to be rather specific, with complete block of αKGDH and only minimal effects on other enzymes that utilize α-ketoglutarate or related α-keto acids (Bunik et al., 2005). Hence, the prevention of the effects of SP by TH indicates that they are indeed due to the dysfunction of αKGDHC. Minor contributions by modulation of another common target or pathway cannot be entirely excluded.

Hyperosmotic sucrose leads to release of glutamate predominantly from the readily releasable pool (RRP) of vesicles, which is responsible for evoked Ca^{2+}-dependent release of glutamate (Rosenmund and Stevens, 1996). Of note, other forms of vesicular glutamate release might also contribute to glutamate excitotoxicity, for example, a spontaneous, Ca^{2+}-independent form of glutamate release. The latter was attributed specifically to a resting pool (RP) of synaptic vesicles by some (e.g. Fredj and Burrone, 2009) but not by other authors (Wilhelm et al., 2010; Duan et al., 2024; Arnold and Peters, 2025). Our sucrose assay of glutamate content does not provide information about glutamate content in pools other than the RRP. However, glutamate has been shown to be loaded into synaptic vesicles in an early stage of vesicular recycling and, once the vesicles have been refilled, they appear to remain relatively inactive in terms of neurotransmitter exchange (Prior and Clague, 1997; Rizzoli, 2014). Hence, the changes we observed upon modulation of αKGDHC might not only apply to the RRP.

By using a cell culture model, we employed a simplified experimental system in our study. Consequently, all conclusions must be interpreted in consideration of the fact that the complexity of a natural biological system might not be perfectly mimicked (Featherstone and Shippy, 2008). However, we used the neuron and glia co-cultures only after at least 12 days in culture, when neurons had fully differentiated on a glial feeder-layer. This system has been shown in our hands to exhibit essential aspects of glutamatergic signal transduction, including glutamate-glutamine cycling between glial cells and neurons (Kubista et al., 2025). Hence, considerable transferability of the results to the *in vivo* situation seems to be warranted.

MATERIALS AND METHODS

Sources of chemicals

Succinyl phosphonate (#MCE-HY-12688A) was from MedChemExpress EU (Sollentuna, Sweden), TH (#T1270), NMDA (#M3262), (S)-AMPA (#A0326), glutamate (#G1251), glycine (#G8790), sucrose (#S9378) and propidium iodide (#P4170) were from Sigma-Aldrich (Vienna, Austria), YM298198 (ab120015) and MTEP (ab120035) were from Abcam (Cambridge, UK), U73122 (#T6243) was from TargetMol (Linz, Austria), Fluo4 AM (#F14201) was from Thermo Fisher Scientific (Waltham, MA, USA), CNQX (#1045) was from Tocris (Dublin, Ireland). Tetrodotoxin (TTX, # L8503) was from Latoxan (Portes-les-Valence, France) and bulk chemicals were from Sigma-Aldrich.

Primary hippocampal neuron and glia co-cultures, and modulation of αKGDHC

Once a week, a pregnant Sprague-Dawley rat was received from Charles River Laboratories (Sulzfeld, Germany). Within 24 h after birth, neonatal animals of both sexes were killed by decapitation in full compliance with the provisions of the Austrian Animal Protection Law; for further information and details of the preparation see Hotka et al. (2020). In brief, hippocampi were dissected and after enzymatic digestion of the tissue for 20 min with papain, cells were dissociated by trituration in culture medium. Cells were seeded on to PDL-coated dishes and cultured for at least 12 days. The growth of glial cells was stopped by addition of cytosine arabinoside (1 µM) 3 days after seeding. SP (200 µM) and TH (1 mM) were added from concentrated aqueous stocks to the culture medium to obtain the desired final concentrations. Cultures were then incubated at 37°C under 5% CO_2 for an additional 36 to 48 h. For experiments, cultures were transferred to standard external solution (SES) which contained (in mM): 140 NaCl, 3 KCl, 2 $CaCl_2$, 2 $MgCl_2$, 10 HEPES, 20 glucose (pH was adjusted to 7.4 by NaOH). In the neuronal viability assays (Figs 1A and 3), all pretreatment conditions were tested in parallel on a total of three independent preparations, with the exception of the control experiment, which served to confirm the viability of the culture and to ensure that the experimental procedure did not cause significant neuronal toxicity (Fig. 1B). In the electrophysiological experiments (Figs 2–7, 8A), typically only one neuron per dish was used (to rule out any effect of a previous experiment on another experiment in the same dish) and care was taken to perform one measurement from each pretreatment condition (ctrl, SP, TH and, if applicable, SP+TH) per experimental day. Hence, data collection in each set of experiments spanned several weeks and involved multiple independent preparations (three to seven). Fluo4 Ca^{2+} measurements (Fig. 8B–E) were performed on cultures of four independent preparations.

Neuronal viability assay

The viability of the neurons was investigated by fluorescence staining of dead cells using propidium iodide (PI) in cultures exposed to SES with various concentrations of glutamate or experiencing 6-h long seizure-like activity induced by nominally Mg^{2+}-free extracellular solution at 37°C. Except for the omission of $MgCl_2$, this 'zero-Mg^{2+}' extracellular solution was identical to the SES. For determination of viability of unstimulated cells, cultures were kept for the same time in SES. For PI staining, cultures were exposed to SES containing 10 µM PI (Fig. S1). For each dish (i.e. biological replicates), four to six microscopic fields of view (FOV), that

is, technical replicates, were analyzed using an Olympus IX70 fluorescence microscope equipped with an Andor EMCCD camera. For each FOV, a brightfield image as well as an image from the red fluorescent protein (RFP) channel were taken. Data were obtained using the open-source image processing software Fiji (Schindelin et al., 2012). Dead cells were counted on the fluorescence image, whereas the number of unstained neurons was determined by visual inspection of the brightfield image onto which the fluorescence image had been superimposed, using a manual cell counter tool. Counting was performed by a researcher who was aware of the experimental conditions. Viability was calculated from the ratio between the number of cells with stained nuclei and the number of these stained cells plus the number of unstained neurons, and is indicated as percentage of viable cells. The *n* numbers in these experiments (Figs 1 and 3) represent the total FOV, which were analyzed in three dishes from three different preparations (i.e. from nine dishes in each experimental condition) in Fig. 1A or in two dishes from three different preparations (i.e. from six dishes in each experimental condition) in Fig. 3.

Electrophysiology

Patch-clamp electrophysiology was used to determine membrane voltage (perforated patch-clamp using amphotericin B) or current responses (whole-cell patch-clamp measurements) to application of increasing concentrations of glutamate, NMDA and AMPA, respectively. Recordings were performed using a Multiclamp 700B amplifier and Clampex software, which is part of the pCLAMP electrophysiology data acquisition and analysis software package (Molecular Devices, Sunnyvale, CA, USA). Patch pipettes were made of borosilicate capillaries (GB150-8P, Science Products, Hofheim, Germany) with a Sutter P97 horizontal puller (Sutter Instrument Company, Novato, CA, USA). Tip resistances lay between 3.5 and 5 MΩ. The pipette solution contained (in mM): 120 potassium gluconate, 1.5 sodium gluconate, 3.5 NaCl, 1.5 $CaCl_2$, 0.25 $MgCl_2$, 10 HEPES, 10 glucose and 5 EGTA. The pH was adjusted to 7.3 by KOH. Electrophysiological experiments were performed at room temperature, and cells were superfused continuously using a DAD-12 drug application system (Adams & List, Westbury, NY, USA) with a micromanifold holding 12 channels converging into a 100 µM diameter quartz outlet (ALA Scientific Instruments, NY, USA). The tip of the outlet was positioned in close proximity (~250 µm) to the patch-clamped cell. Cells were superfused with SES or glutamate-, AMPA-, and NMDA-containing SES via different reservoirs of the DAD-12 system. AMPA- and NMDA-containing SES also contained 0.5 µM tetrodotoxin (TTX), and NMDA-containing SES was additionally supplemented with 10 µM glycine. Currents measured in voltage-clamp experiments are shown in a form normalized to the membrane capacitance (as a proxy for the cell size) and are therefore scaled using the term 'current density' or, if the current maxima were evaluated, as 'peak current density' with the unit pA/pF.

Discharge dynamics across the different pretreatment groups were assessed through systematic, expert-guided visual inspection of current-clamp recordings standardized in time and amplitude. This multiparametric evaluation approach enabled the simultaneous consideration of all measurable aspects, ensuring a comprehensive representation of the diverse firing behaviors present within the neuronal population.

Sucrose shock assay

Glutamate content of synaptic vesicles was determined via whole-cell patch-clamp measurement of the postsynaptic currents induced by sucrose (500 mM) shock (Rosenmund and Stevens, 1996). Neurons were voltage-clamped to −70 mV. Sucrose shock-induced release of synaptic vesicles was elicited by switching the superfusing solution from SES to high sucrose containing solution in the presence of 0.5 µM TTX. The postsynaptic currents were mediated by AMPA receptors as revealed by their sensitivity to 6-cyano-7-nitroquinoxaline-2,3-dione disodium salt (CNQX) as shown in Fig. S3.

Fluo4 Ca^{2+} measurements

Cells were loaded with 1 µM Fluo4 AM (Thermo Fisher Scientific) in culture medium for 15 min at 37°C followed by washout with SES. An excitation wavelength of 488 nm and a detection wavelength of 525 nm were used for imaging. As in the electrophysiological experiments, cells were continuously superfused using a DAD-8 drug application system. TTX (0.5 µM) and the PLC inhibitor U73122 were present in the bath SES as well as in the superfusion SES to avoid network effects as well as acute activation of type 1 mGluR receptors by application of glutamate. Neurons were imaged using 20× objective magnification and two fields of view were analyzed per culture dish. Fluo 4 AM fluorescence was analyzed in ImageJ (Schneider et al., 2012) as a mean fluorescence obtained from circular regions of interest positioned over neuronal somata. Individual fluorescence traces were averaged and statistically analyzed in Graphpad Prism 10.

Statistics

Statistical comparisons were made using GraphPad Prism software (Boston, MA, USA; version 10.5.0) by ordinary one-way ANOVA in combination with Tukey's multiple comparisons post hoc test or – in cases where evidence for normal distribution was not obtained using Kolmogorov–Smirnov test or d'Agostino and Pearson test – by Kruskal–Wallis test in combination with Dunn's multiple comparisons post hoc test (Figs 5B, 8D,E). Nonlinear regression–derived EC_{50} values from the concentration–response data in Fig. 4D were statistically assessed using the GraphPad comparison of fits procedure. Significance is indicated as $*P<0.05$, $**P<0.01$, $***P<0.001$ or $****P<0.0001$. A lack of statistical significance is indicated by ns (not significant). Graphical illustrations were also created using GraphPad Prism.

Acknowledgements

The technical assistance by Tanja Wagner and Elena Lilliu is gratefully acknowledged.

Competing interests

The authors declare no competing or financial interests.

Author contributions

Conceptualization: H.K., M.H., A.V.K.; Data curation: V.G., M.H., B.H.; Formal analysis: V.G., M.H.; Funding acquisition: H.K., M.H., A.V.K.; Investigation: V.G., M.H.; Methodology: H.K., M.H., B.H.; Project administration: H.K., M.H.; Supervision: H.K., M.H., K.H., S.B., A.V.K.; Writing – original draft: H.K., M.H., S.B.; Writing – review & editing: H.K., M.H., V.G., K.H., S.B., A.V.K.

Funding

This research was funded in whole or in part by the Austrian Science Fund (FWF) (P36145 to H.K., PAT8605623 to M.H. and P33799 to A.V.K.]. Open Access funding provided by Medical University of Vienna and the Austrian Science Fund (FWF). Deposited in PMC for immediate release.

Data and resource availability

All relevant data and details of resources can be found within this article and its supplementary information.

Peer review history

The peer review history is available online at https://journals.biologists.com/jcs/lookup/doi/10.1242/jcs.264420.reviewer-comments.pdf

References

Alcoreza, O. B., Patel, D. C., Tewari, B. P. and Sontheimer, H. (2021). Dysregulation of ambient glutamate and glutamate receptors in epilepsy: an astrocytic perspective. *Front. Neurol.* **12**, 652159. doi:10.3389/fneur.2021.652159

Arnold, R. A. and Peters, J. H. (2025). Functionally distinct evoked and spontaneous neurotransmission operate via a shared pool of synaptic vesicles in viscerosensory afferents. *J. Physiol.* **603**, 3141-3159. doi:10.1113/JP288301

Banke, T. G. and Lambert, J. D. C. (1999). Novel potent AMPA analogues differentially affect desensitisation of AMPA receptors in cultured hippocampal neurons. *Eur. J. Pharmacol.* **367**, 405-412. doi:10.1016/S0014-2999(98)00975-3

Belov Kirdajova, D., Kriska, J., Tureckova, J. and Anderova, M. (2020). Ischemia-triggered glutamate excitotoxicity from the perspective of glial cells. *Front. Cell Neurosci.* **14**, 51. doi:10.3389/fncel.2020.00051

Benquet, P., Gee, C. E. and Gerber, U. (2002). Two distinct signaling pathways upregulate NMDA receptor responses via two distinct metabotropic glutamate receptor subtypes. *J. Neurosci.* **22**, 9679-9686. doi:10.1523/JNEUROSCI.22-22-09679.2002

Bunik, V. I., Denton, T. T., Xu, H., Thompson, C. M., Cooper, A. J. L. and Gibson, G. E. (2005). Phosphonate analogues of alpha-ketoglutarate inhibit the activity

of the alpha-ketoglutarate dehydrogenase complex isolated from brain and in cultured cells. *Biochemistry* **44**, 10552-10561. doi:10.1021/bi0503100

Bunik, V. I., Kabysheva, M. S., Klimuk, E. I., Storozhevykh, T. P. and Pinelis, V. G. (2009). Phosphono analogues of 2-oxoglutarate protect cerebellar granule neurons upon glutamate excitotoxicity. *Ann. N. Y. Acad. Sci.* **1171**, 521-529. doi:10.1111/j.1749-6632.2009.04709.x

Divakaruni, A. S., Wallace, M., Buren, C., Martyniuk, K., Andreyev, A. Y., Li, E., Fields, J. A., Cordes, T., Reynolds, I. J., Bloodgood, B. L. et al. (2017). Inhibition of the mitochondrial pyruvate carrier protects from excitotoxic neuronal death. *J. Cell Biol.* **216**, 1091-1105. doi:10.1083/jcb.201612067

Duan, J., Kahms, M., Steinhoff, A. and Klingauf, J. (2024). Spontaneous and evoked synaptic vesicle release arises from a single releasable pool. *Cell Rep.* **43**, 114461. doi:10.1016/j.celrep.2024.114461

Featherstone, D. E. and Shippy, S. A. (2008). Regulation of synaptic transmission by ambient extracellular glutamate. *Neuroscientist* **14**, 171-181. doi:10.1177/1073858407308518

Fitzjohn, S. M., Irving, A. J., Palmer, M. J., Harvey, J., Lodge, D. and Collingridge, G. L. (1996). Activation of group I mGluRs potentiates NMDA responses in rat hippocampal slices. *Neurosci. Lett.* **203**, 211-213. doi:10.1016/0304-3940(96)12301-6

Fredj, N. B. and Burrone, J. (2009). A resting pool of vesicles is responsible for spontaneous vesicle fusion at the synapse. *Nat. Neurosci.* **12**, 751-758. doi:10.1038/nn.2317

Fukushima, K., Tabata, Y., Imaizumi, Y., Kohmura, N., Sugawara, M., Sawada, K., Yamazaki, K. and Ito, M. (2014). Characterization of human hippocampal neural stem/progenitor cells and their application to physiologically relevant assays for multiple ionotropic glutamate receptors. *J. Biomol. Screen.* **19**, 1174-1184. doi:10.1177/1087057114541149

Gao, S., Zhu, Z. and Zheng, W. (2025). Thiamine administration and in-hospital mortality in patients with traumatic brain injury: analysis of the MIMIC-IV database. *Front. Neurol.* **16**, 1448439. doi:10.3389/fneur.2025.1448439

Grienberger, C., Chen, X. and Konnerth, A. (2014). NMDA receptor-dependent multidendrite Ca^{2+} spikes required for hippocampal burst firing in vivo. *Neuron* **81**, 1274-1281. doi:10.1016/j.neuron.2014.01.014

Hamada, S., Hirashima, H., Imaeda, M., Okamoto, Y., Hamaguchi-Hamada, K. and Kurumata-Shigeto, M. (2013). Thiamine deficiency induces massive cell death in the olfactory bulbs of mice. *J. Neuropathol. Exp. Neurol.* **72**, 1193-1202. doi:10.1097/NEN.0000000000000017

Hansen, G. E. and Gibson, G. E. (2022). The α-ketoglutarate dehydrogenase complex as a hub of plasticity in neurodegeneration and regeneration. *Int. J. Mol. Sci.* **23**, 12403. doi:10.3390/ijms232012403

Heidinger, V., Manzerra, P., Wang, X. Q., Strasser, U., Yu, S.-P., Choi, D. W. and Behrens, M. M. (2002). Metabotropic glutamate receptor 1-induced upregulation of NMDA receptor current: mediation through the Pyk2/Src-family kinase pathway in cortical neurons. *J. Neurosci.* **22**, 5452-5461. doi:10.1523/JNEUROSCI.22-13-05452.2002

Herman, M. A. and Jahr, C. E. (2007). Extracellular glutamate concentration in hippocampal slice. *J. Neurosci.* **27**, 9736-9741. doi:10.1523/JNEUROSCI.3009-07.2007

Hosmann, A., Milivojev, N., Dumitrescu, S., Reinprecht, A., Weidinger, A. and Kozlov, A. V. (2021). Cerebral nitric oxide and mitochondrial function in patients suffering aneurysmal subarachnoid hemorrhage-a translational approach. *Acta Neurochir. (Wien)* **163**, 139-149. doi:10.1007/s00701-020-04536-x

Hotka, M., Cagalinec, M., Hilber, K., Hool, L., Boehm, S. and Kubista, H. (2020). L-type Ca^{2+} channel-mediated Ca^{2+} influx adjusts neuronal mitochondrial function to physiological and pathophysiological conditions. *Sci. Signal.* **13**, eaaw6923. doi:10.1126/scisignal.aaw6923

Hou, Z. and Brenner, J. S. (2024). Developing targeted antioxidant nanomedicines for ischemic penumbra: Novel strategies in treating brain ischemia-reperfusion injury. *Redox. Biol.* **73**, 103185. doi:10.1016/j.redox.2024.103185

Kabysheva, M. S., Storozhevykh, T. P., Pinelis, V. G. and Bunik, V. I. (2009). Synthetic regulators of the 2-oxoglutarate oxidative decarboxylation alleviate the glutamate excitotoxicity in cerebellar granule neurons. *Biochem. Pharmacol.* **77**, 1531-1540. doi:10.1016/j.bcp.2009.02.001

Kohara, A., Takahashi, M., Yatsugi, S.-I., Tamura, S., Shitaka, Y., Hayashibe, S., Kawabata, S. and Okada, M. (2008). Neuroprotective effects of the selective type 1 metabotropic glutamate receptor antagonist YM-202074 in rat stroke models. *Brain Res.* **1191**, 168-179. doi:10.1016/j.brainres.2007.11.035

Kovac, S., Domijan, A.-M., Walker, M. C. and Abramov, A. Y. (2012). Prolonged seizure activity impairs mitochondrial bioenergetics and induces cell death. *J. Cell Sci.* **125**, 1796-1806. doi:10.1242/jcs.099176

Kubista, H., Gentile, F., Schicker, K., Köcher, T., Boehm, S. and Hotka, M. (2025). Mitochondrial glutamine metabolism drives epileptogenesis in primary hippocampal neurons. *J. Neurosci.* **45**, e0110252025. doi:10.1523/JNEUROSCI.0110-25.2025

Lai, T. K. Y., Zhai, D., Su, P., Jiang, A., Boychuk, J. and Liu, F. (2019). The receptor-receptor interaction between mGluR1 receptor and NMDA receptor: a potential therapeutic target for protection against ischemic stroke. *FASEB J.* **33**, 14423-14439. doi:10.1096/fj.201900417R

Lan, J.-Y., Skeberdis, V. A., Jover, T., Zheng, X., Bennett, M. V. L. and Zukin, R. S. (2001). Activation of metabotropic glutamate receptor 1 accelerates NMDA receptor trafficking. *J. Neurosci.* **21**, 6058-6068. doi:10.1523/JNEUROSCI.21-16-06058.2001

Lewerenz, J. and Maher, P. (2015). Chronic glutamate toxicity in neurodegenerative diseases-what is the evidence? *Front. Neurosci.* **9**, 469. doi:10.3389/fnins.2015.00469

Li, H., Zhang, N., Sun, G. and Ding, S. (2013). Inhibition of the group I mGluRs reduces acute brain damage and improves long-term histological outcomes after photothrombosis-induced ischaemia. *ASN Neuro.* **5**, 195-207. doi:10.1042/AN20130002

Mahmoud, S., Gharagozloo, M., Simard, C. and Gris, D. (2019). Astrocytes maintain glutamate homeostasis in the CNS by controlling the balance between glutamate uptake and release. *Cells* **8**, 184. doi:10.3390/cells8020184

McKenna, M. C. (2007). The glutamate-glutamine cycle is not stoichiometric: fates of glutamate in brain. *J. Neurosci. Res.* **85**, 3347-3358. doi:10.1002/jnr.21444

Meyer, C., Kettner, A., Hochenegg, U., Rubi, L., Hilber, K., Koenig, X., Boehm, S., Hotka, M. and Kubista, H. (2021). On the origin of paroxysmal depolarization shifts: the contribution of Cav1.x channels as the common denominator of a polymorphous neuronal discharge pattern. *Neuroscience* **468**, 265-281. doi:10.1016/j.neuroscience.2021.05.011

Mukhin, A., Fan, L. and Faden, A. I. (1996). Activation of metabotropic glutamate receptor subtype mGluR1 contributes to post-traumatic neuronal injury. *J. Neurosci.* **16**, 6012-6020. doi:10.1523/JNEUROSCI.16-19-06012.1996

Mukhin, A. G., Ivanova, S. A. and Faden, A. I. (1997). mGluR modulation of post-traumatic neuronal death: role of NMDA receptors. *Neuroreport* **8**, 2561-2566. doi:10.1097/00001756-199707280-00028

Murotomi, K., Takagi, N., Takayanagi, G., Ono, M., Takeo, S. and Tanonaka, K. (2008). mGluR1 antagonist decreases tyrosine phosphorylation of NMDA receptor and attenuates infarct size after transient focal cerebral ischemia. *J. Neurochem.* **105**, 1625-1634. doi:10.1111/j.1471-4159.2008.05260.x

Nardone, R., Höller, Y., Storti, M., Christova, M., Tezzon, F., Golaszewski, S., Trinka, E. and Brigo, F. (2013). Thiamine deficiency induced neurochemical, neuroanatomical, and neuropsychological alterations: a reappraisal. *ScientificWorldJournal* **2013**, 309143. doi:10.1155/2013/309143

Nedergaard, M., Takano, T. and Hansen, A. J. (2002). Beyond the role of glutamate as a neurotransmitter. *Nat. Rev. Neurosci.* **3**, 748-755. doi:10.1038/nrn916

Olney, J. W. (1971). Glutamate-induced neuronal necrosis in the infant mouse hypothalamus. An electron microscopic study. *J. Neuropathol. Exp. Neurol.* **30**, 75-90. doi:10.1097/00005072-197101000-00008

Prior, I. A. and Clague, M. J. (1997). Glutamate uptake occurs at an early stage of synaptic vesicle recycling. *Curr. Biol.* **7**, 353-356. doi:10.1016/S0960-9822(06)00159-X

Rizzoli, S. O. (2014). Synaptic vesicle recycling: steps and principles. *EMBO J.* **33**, 788-822. doi:10.1002/embj.201386357

Rosenmund, C. and Stevens, C. F. (1996). Definition of the readily releasable pool of vesicles at hippocampal synapses. *Neuron* **16**, 1197-1207. doi:10.1016/S0896-6273(00)80146-4

Schindelin, J., Arganda-Carreras, I., Frise, E., Kaynig, V., Longair, M., Pietzsch, T., Preibisch, S., Rueden, C., Saalfeld, S., Schmid, B. et al. (2012). Fiji: an open-source platform for biological-image analysis. *Nat. Methods* **9**, 676-682. doi:10.1038/nmeth.2019

Schneider, C. A., Rasband, W. S. and Eliceiri, K. W. (2012). NIH Image to ImageJ: 25 years of image analysis. *Nat. Methods* **9**, 671-675. doi:10.1038/nmeth.2089

Skeberdis, V. A., Lan, J., Opitz, T., Zheng, X., Bennett, M. V. L. and Zukin, R. S. (2001). mGluR1-mediated potentiation of NMDA receptors involves a rise in intracellular calcium and activation of protein kinase C. *Neuropharmacology* **40**, 856-865. doi:10.1016/S0028-3908(01)00005-3

Starkov, A. A. (2013). An update on the role of mitochondrial α-ketoglutarate dehydrogenase in oxidative stress. *Mol. Cell. Neurosci.* **55**, 13-16. doi:10.1016/j.mcn.2012.07.005

Tani, H., Dulla, C. G., Farzampour, Z., Taylor-Weiner, A., Huguenard, J. R. and Reimer, R. J. (2014). A local glutamate-glutamine cycle sustains synaptic excitatory transmitter release. *Neuron* **81**, 888-900. doi:10.1016/j.neuron.2013.12.026

Teplov, I. Y., Zinchenko, V. P., Kosenkov, A. M., Gaidin, S. G., Nenov, M. N. and Sergeev, A. I. (2021). Involvement of NMDA and GABA(A) receptors in modulation of spontaneous activity in hippocampal culture: interrelations between burst firing and intracellular calcium signal. *Biochem. Biophys. Res. Commun.* **553**, 99-106. doi:10.1016/j.bbrc.2021.02.149

Tora, A. S., Rovira, X., Cao, A.-M., Cabayé, A., Olofsson, L., Malhaire, F., Scholler, P., Baik, H., Van Eeckhaut, A., Smolders, I. et al. (2018). Chloride ions stabilize the glutamate-induced active state of the metabotropic glutamate receptor 3. *Neuropharmacology* **140**, 275-286. doi:10.1016/j.neuropharm.2018.08.011

Wang, J., Wang, F., Mai, D. and Qu, S. (2020). Molecular mechanisms of glutamate toxicity in Parkinson's disease. *Front. Neurosci.* **14**, 585584. doi:10.3389/fnins.2020.585584

Wang, R., Zeng, Y., Xu, J. and He, M. (2024). Thiamine use is associated with better outcomes for traumatic brain injury patients. *Front. Nutr.* **11**, 1362817. doi:10.3389/fnut.2024.1362817

Weidinger, A., Milivojev, N., Hosmann, A., Duvigneau, J. C., Szabo, C., Törö, G., Rauter, L., Vaglio-Garro, A., Mkrtchyan, G. V., Trofimova, L. et al. (2023). Oxoglutarate dehydrogenase complex controls glutamate-mediated neuronal death. *Redox Biol.* **62**, 102669. doi:10.1016/j.redox.2023.102669

Wilhelm, B. G., Groemer, T. W. and Rizzoli, S. O. (2010). The same synaptic vesicles drive active and spontaneous release. *Nat. Neurosci.* **13**, 1454-1456. doi:10.1038/nn.2690